Available online at www.sciencedirect.com
ScienceDirect
Trans. Nonferrous Met. Soc. China 25(2015) 2103−2112
Transactions of Nonferrous Metals Society of China
www.tnmsc.cn

Microstructure and mechanical properties of Mg, Ag and Zn multi-microalloyed Al−(3.2−3.8)Cu−(1.0−1.4)Li alloys

Jin-feng LI[1], Ping-li LIU[1], Yong-lai CHEN[2], Xu-hu ZHANG[2], Zi-qiao ZHENG[1]

1. School of Materials Science and Engineering, Central South University, Changsha 410083, China;
2. Aerospace Research Institute of Materials and Processing Technology, Beijing 100076, China

Received 22 September 2014; accepted 28 December 2014

Abstract: To develop super-high strength Al−Li alloy, the microstructures and mechanical properties of Mg, Ag and Zn micro-alloyed Al−(3.2−3.8)Cu−(1.0−1.4)Li alloys (mass fraction) with T8 temper were studied. The results showed that 1% of lower Li content restricted the strengthening effect of increasing Cu content, while simultaneous increase in Cu and Li contents contributed effectively to the enhancement of strength. The alloys were mainly strengthened by plenty of fine and well dispersed $T1(Al_2CuLi)$ precipitates. There were also some minor precipitates of $\theta'(Al_2Cu)$ and $\delta'(Al_3Li)$, which became less in number density, even disappeared during the aging process. Meanwhile, higher Li content favored the formation θ' and δ' and a small amount of $S'(Al_2CuMg)$ phases. In addition, strengthening effect and microstructure variation were analyzed through total non-solution mole fraction of Cu and Li and their mole ratio. To obtain Al−Li alloy with super-high strength, the total mole fractions of Cu and Li should be increased, and their mole ratios should also be kept at a certain high level.
Key words: Al−Li alloy; precipitate; Cu/Li mole ratio; microstructure; mechanical properties

1 Introduction

Al−Cu−Li alloys were considered the most attractive alloys in the aircraft and aerospace industries because of their desirable properties, such as low density, high specific strength and elastic modulus, good corrosion resistance, excellent cryogenic properties, and low fatigue crack growth rate [1−3]. In fact, the third generation Al−Li alloys, such as alloys 2195, 2050, 2099, 2196 and 2197 were successfully used and performed excellently in aircraft and aerospace structures [4].

An important method to improve the performance of Al−Li alloys is to add micro-alloying elements, such as Mg, Ag, Mn and Zn. Research on micro-alloying in Al−Li alloys has therefore gotten more and more attractive. It was reported that combined addition of Mg and Ag to Al−Li alloys powerfully promoted the uniform formation of $T1(Al_2CuLi)$ precipitates with much smaller size, but single addition of Ag displayed little effect on their precipitation [5]. The combined addition of Mg and Ag therefore greatly enhanced the strength of Al−Li alloys. The representative Al−Li alloys containing Mg and Ag micro-alloying elements included alloys 2195 and 2050. Al−Li alloy 2195 has been successfully applied in the super lightweight tank of the space shuttle [6], while Al−Li alloy 2050 has recently entered industrial production for various commercial aircrafts as a replacement of alloy 7050 [7]. The combined addition of Mg and Zn showed a similar function as the combined addition of Mg and Ag [8]. The corresponding Mg and Zn micro-alloyed Al−Li alloys included alloys 2099 and 2199 which were used as structural components in Airbus A380. In 2012, RIOJA et al [4,9] developed a new Al−Li alloy 2055, which contained micro-alloying elements of Mg, Ag and Zn simultaneously and exhibited super-high strength and some other excellent performance. Our previous research results also indicated that combined addition of Mg, Ag and Zn displayed better strengthening effect than that of Mg and Ag (or Zn) [10]. This implied that combined addition of Mg, Ag and Zn micro-alloying elements would be an important way to develop Al−Li alloys with super-high strength.

Foundation item: Project (2013AA032401) supported by the National High-tech Research and Development Program of China; Project (2013JSJJ 001) supported by Teacher's Research Foundation of Central South University, China
Corresponding author: Jin-feng LI; Tel: +86-731-88879341; E-mail: lijinfeng@csu.edu.cn
DOI: 10.1016/S1003-6326(15)63821-3

As the main alloying elements in Al−Cu−Li alloys, Cu and Li contents are important factors for developing new Al−Li alloys. They not only provide solid solution strengthening effect, but also enable the formation of some effective hardening precipitates like $T1(Al_2CuLi)$, $\delta'(Al_3Li)$, $\theta'(Al_2Cu)$ and $S'(Al_2CuMg)$. It was reported that the perfect Cu content was 2%−5% (mass fraction, similarly hereinafter) for good strength, ductility and fracture toughness combinations [11]. Li element contributed to a certain hardening effect from the δ' and $T1$ precipitates. HAGIWARA et al [12] found that the addition of Li to Al alloy 2219 caused a continual enhancement in strength with Li content increasing up to 1.25%. Furthermore, KUMAR and HEUBAUM [13] and GUPTA et al [14] reported that some Weldalite 049 Al−Li alloys containing ~1.3% Li exhibited desirable combinations of strength and toughness and that a decrease in strength occurred gradually with Li content higher than 1.3%. Besides, $T1$ precipitate in Al−Li alloys was the most effective strengthening phase, which precipitated along the {111} plane of the Al matrix [15]. Variation of Cu and Li contents would greatly impact the type and volume fraction of precipitates in Al−Li alloys, changing their microstructure and strength. Therefore, it is important to investigate the contents of Cu and Li for developing super-high strength Al−Li alloys.

In this case, as an exploration for super-high strength Al−Li alloys micro-alloyed by Mg, Ag and Zn, the influence of Cu and Li contents on strength was researched, and their microstructures were observed. Meanwhile, the strength variation was analyzed through the total mole fraction of Cu and Li and their ratio.

2 Experimental

Seven Al−Cu−Li alloys with different Cu and Li contents were prepared. Their Cu and Li contents are shown in Table 1. It should be emphasized that all these alloys contain the same micro-alloying elements of 0.4% Mg, 0.4% Ag, 0.4% Zn, 0.3% Mn and 0.12% Zr.

Table 1 Cu and Li contents of experimental Al−Cu−Li alloys

Alloy No.	Mass fraction/%	
	Cu	Li
1	3.24	0.96
2	3.41	0.98
3	3.66	1.00
4	3.77	0.96
5	3.58	1.18
6	3.66	1.38
7	3.48	1.44

After a two-step homogenization treatment, the Al−Cu−Li alloy ingots were rolled to sheets with 2 mm in thickness through hot rolling and cold rolling processes. The sheets were then subjected to a simple T8 aging treatment after solid solution treatment at 520 °C and quenching in water at room temperature. The T8 aging treatment was an artificial aging treatment at 160 °C after 6% pre-deformation through cold rolling.

Tensile specimens with a parallel section gauged 30 mm in length and 8 mm in width were cut down from the T8-treated sheets along the rolling direction, according to the National Standard GB/T228.1−2010. Tensile tests were carried out on an MTS testing machine (MTS858 Mini Bionix II, USA) at a tensile rate of 2 mm/min. The microstructure was observed using a TecnaiG^2 20 ST transmission electron microscope (TEM). The TEM samples were prepared by a twin-jet electro-polishing device in a solution of 75% methanol and 25% nitric acid at −40 to −20 °C with a voltage of 15−30 V and a current of 70−95 mA.

3 Results and discussion

3.1 Mechanical properties of alloys with different Cu and Li contents

The strength and elongation versus aging time curves of ~1.0% Li-containing alloys (Alloys 1−4) with different Cu contents are shown in Fig. 1. At the early aging stage, the tensile strength increases rapidly. After reaching the peak strength, it decreases only a little within the total aging time of 120 h (Fig. 1(a)). The yield strength curves of these four alloys display the same tendency (Fig. 1(b)). As the Cu content is increased from 3.24% to 3.41%, the strength is enhanced obviously. However, as the Cu content is further increased to 3.77%, there is little difference in strength. For Alloys 2, 3 and 4, the peak tensile strength is very close to each other (570−580 MPa). Figure 1(c) shows the elongation of these four alloys as a function of aging time. It is clear that the elongation decreases as the aging time is extended. With Cu content increasing, the elongation lowers as well, but all these four alloys possess an elongation higher than 8%.

Alloys 3, 5 and 6 were designed to explore the effect of increasing Li content on the mechanical properties. In these three alloys, the Cu content is kept at 3.6%−3.7% as far as possible, while Li content is increased from 1.00% (Alloy 3) to 1.18% (Alloy 5) and 1.38% (Alloy 6). Figure 2 shows their strength and elongation as a function of aging time. With increasing Li content, the strength is enhanced step by step. The peak tensile strength and yield strength of Alloy 6 with 3.66% Cu and 1.38% Li are enhanced to 623 MPa and 584 MPa, respectively. The elongation of the above three

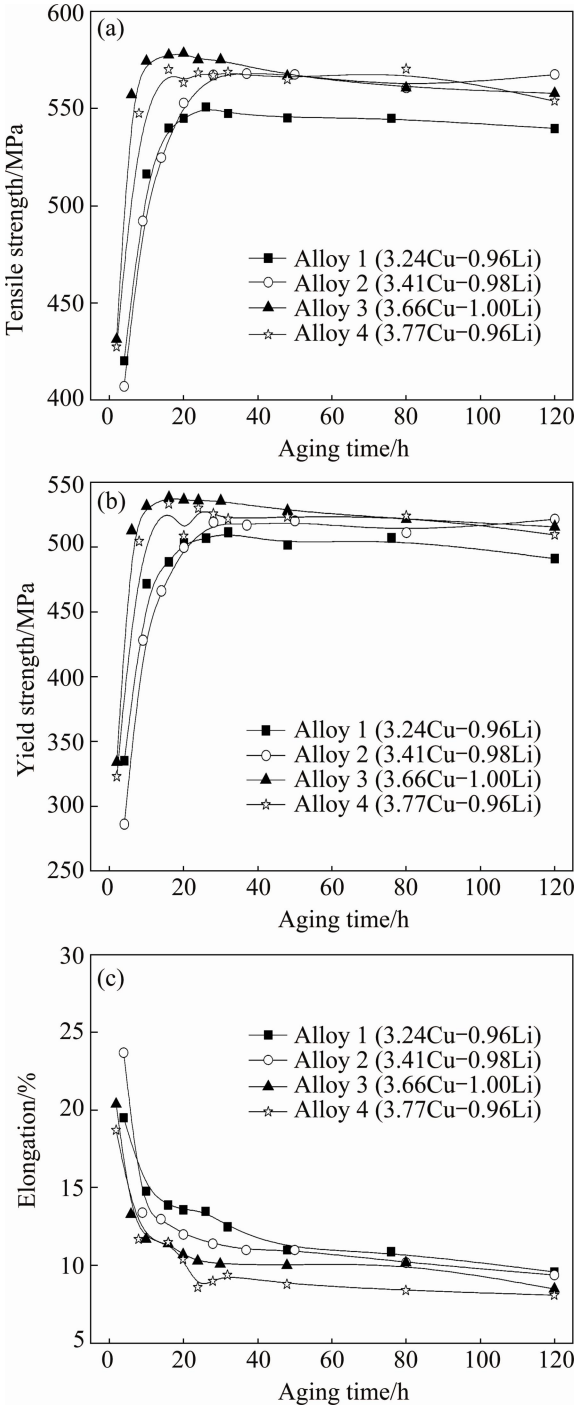

Fig. 1 Tensile strength (a), yield strength (b) and elongation (c) of ~1.0% Li-containing alloys (Alloys 1−4) with different Cu contents as function of aging time

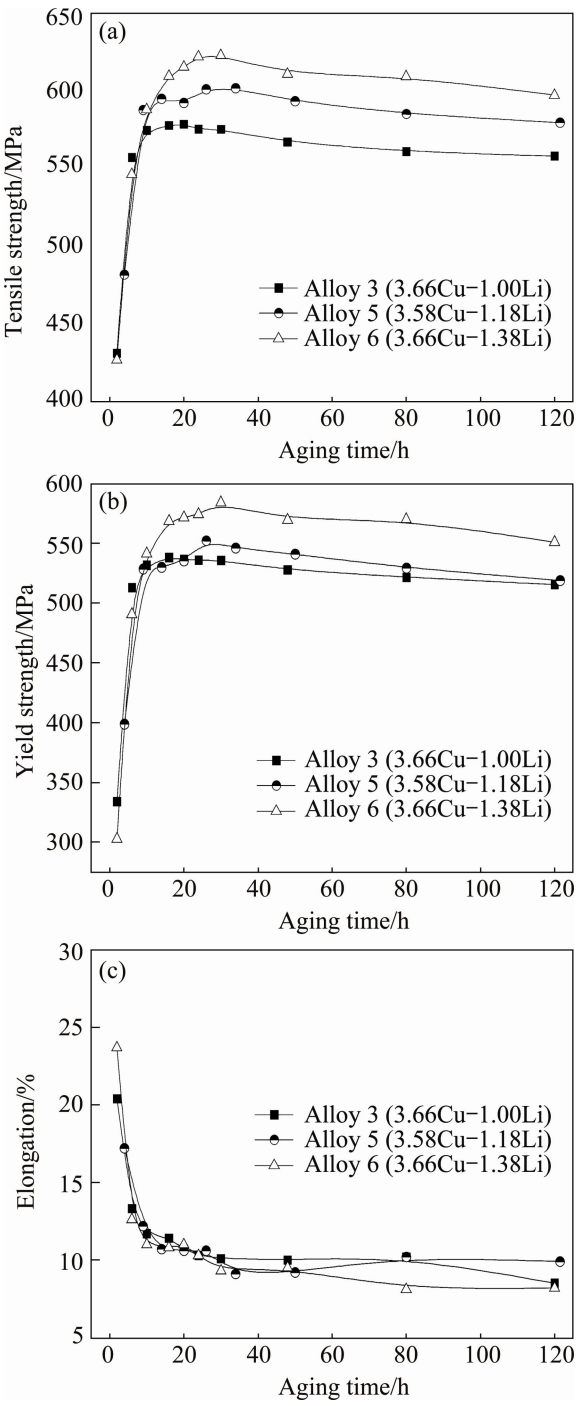

Fig. 2 Tensile strength (a), yield strength (b) and elongation (c) of 3.6%−3.7% Cu-containing alloys (Alloys 3, 5, 6) with different Li contents as function of aging time

alloys is within a certain region ranging from 8% to 11% after 16 h aging (Fig. 2(c)). There is only a little decrease in elongation with increasing Li content.

The above results indicate that lower content of 1.0% Li restricts the strengthening effect of increasing Cu content, while the increase in Li content effectively enhances the strength. Actually, it is also found that simultaneously increasing Cu content from 3.2% to 3.8% and Li content from ~1.0% to ~1.4% is more favourable to the strength enhancement. This dependence can be verified by the strength variation of Alloys 2, 6 and 7. For Alloys 2 and 7, their Cu content is about 3.45%. For Alloys 6 and 7, their Li content is about 1.4%. As shown in Fig. 3, the peak tensile strength increases from nearly 570 MPa (Alloy 2) to 600 MPa (Alloy 7) when Li content is increased from 0.98% to 1.44%, while it increases from 600 MPa (Alloy 7) to 623 MPa (Alloy 6) when Cu content is increased from 3.48% to 3.66%.

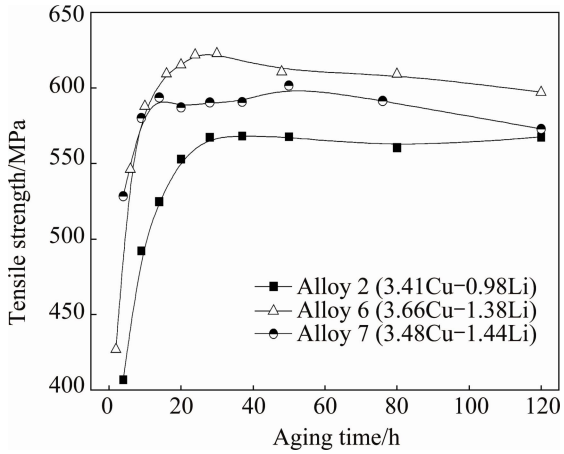

Fig. 3 Tensile strength of Alloys 2, 6 and 7 as function of aging time

3.2 Microstructures of alloys

The TEM images of the alloys in the early under-aging stage are shown in Fig. 4. Alloy 1 under-aging for 4 h reveals the $T1$ and δ' spots and weak θ' streaks in the selected area diffraction (SAD) pattern from a [100] zone axis (Fig. 4(a)). That is to say, $T1$, δ' and θ' phases are precipitated in the early under-aging stage. Alloy 3 with under-aging for 2 h presents the similar SAD pattern (Fig. 4(c)). Dark field (DF) TEM images in Figs. 4(b) and (d) show the very fine $T1$ precipitates, of which the size is 40−50 nm and 20−30 nm in length, respectively. It is therefore concluded that these experimental alloys experience the precipitation process of $T1$, θ' and δ' phases in the early aging stage.

Figures 5−7 give the SAD patterns and some TEM images of the near peak-aged 1.0% Li-containing alloys (Alloys 1−4) with different Cu contents. The SAD patterns from [112] zone axis indicate that obvious $T1$ precipitates exist in these four alloys (Fig. 5(a), Fig. 6(a), Figs. 7(a) and (d)). Considerable $T1$ precipitates are indeed observed in Alloy 1 with 3.24% Cu (Fig. 5(c)). However, for Alloy 1, no obvious δ' spots and θ' streaks appear in the SAD pattern from [100] zone axis (Fig. 5(b)), indicating no obvious δ' and θ' phases in the near peak-aging stage. The SAD pattern from [100] zone axis for Alloy 2 with 3.41% Cu shows apparent $T1$ spots,

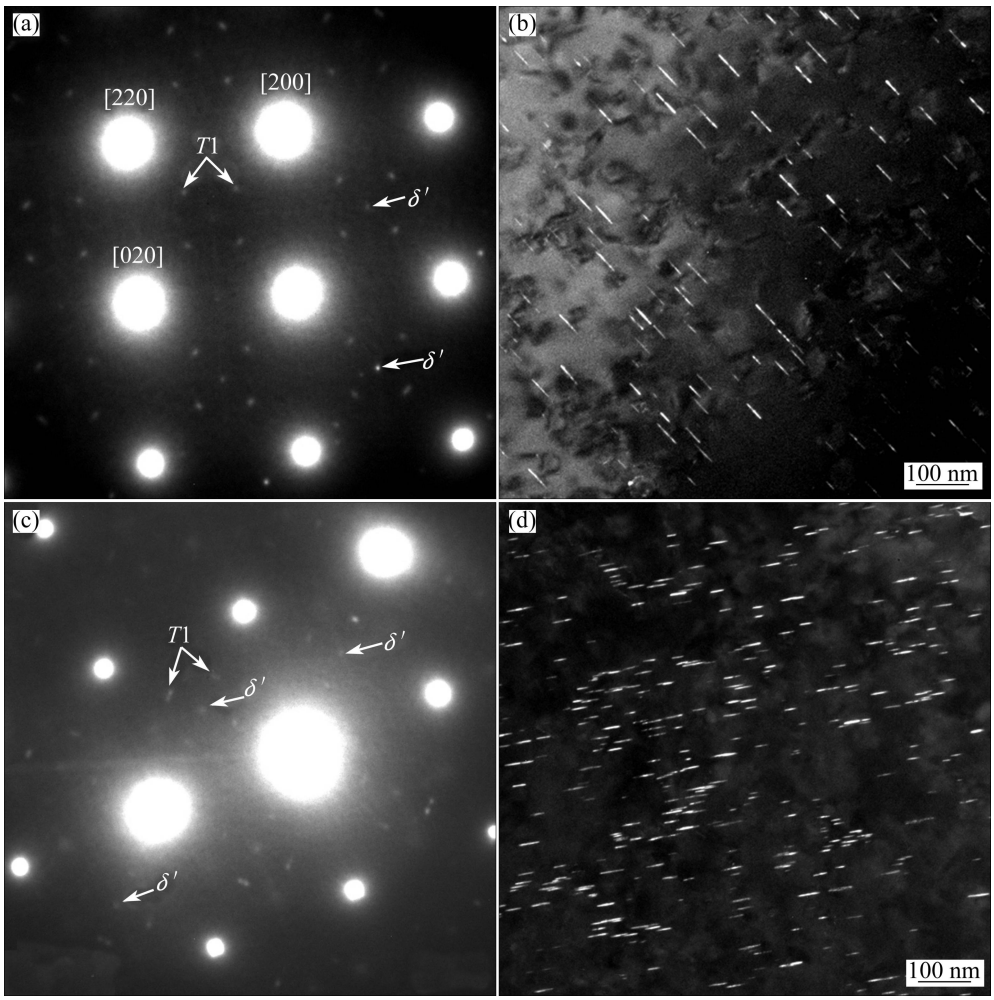

Fig. 4 SAD patterns of $[100]_{Al}$ (a,c) and DF TEM images of $[112]_{Al}$ (b,d) showing $T1$ precipitates: (a,b) Alloy 1 aged for 4 h; (c,d) Alloy 3 aged for 2 h

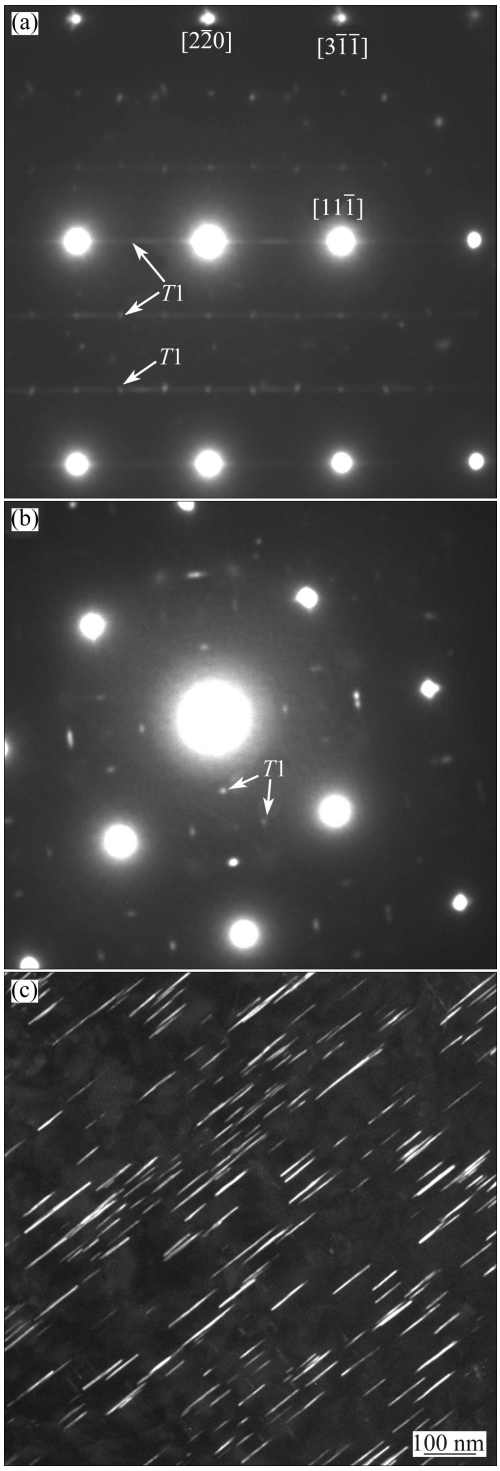

Fig. 5 SAD patterns (a,b) and DF TEM image (c) of Alloy 1 aged for 26 h: (a) $[112]_{Al}$ SAD pattern; (b) $[100]_{Al}$ SAD pattern; (c) $[112]_{Al}$ DF TEM image showing $T1$ precipitates

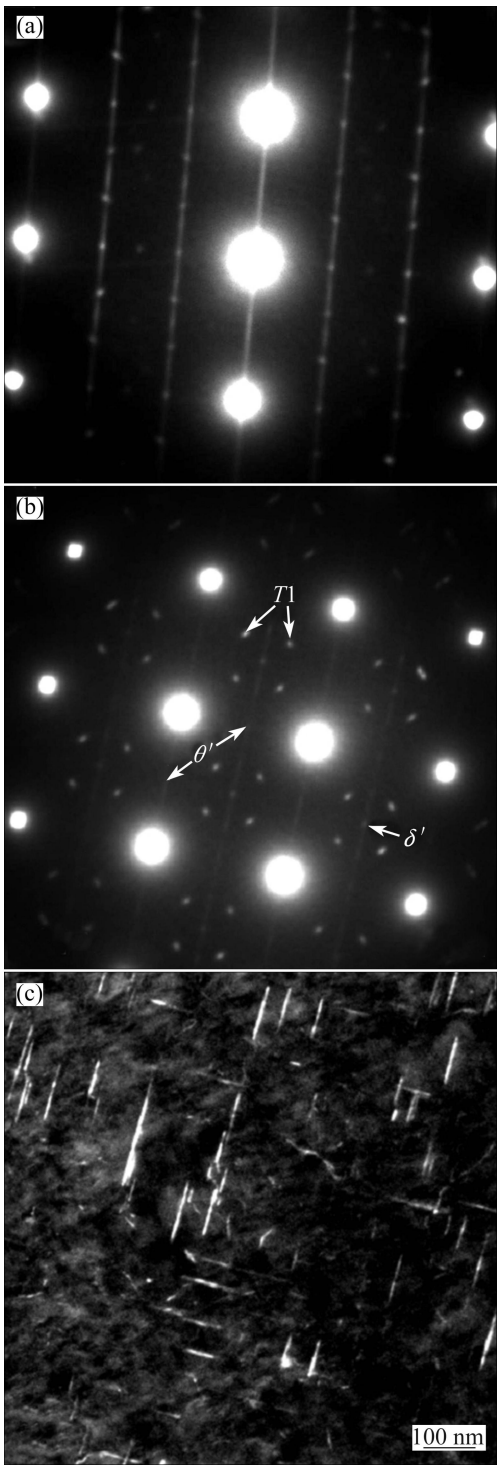

Fig. 6 SAD patterns (a,b) and DF TEM image (c) of Alloy 2 aged for 37 h: (a) $[112]_{Al}$ SAD pattern; (b) $[100]_{Al}$ SAD pattern; (c) $[100]_{Al}$ DF TEM image showing θ' precipitates

weak θ' steaks and δ' spots (Fig. 6(b)). That is to say, there exist a variety of $T1$ precipitates and some θ' and δ' precipitates in Alloy 2, and the corresponding θ' precipitates are observed in Fig. 6(c). The similar microstructural characteristics are observed in Alloy 3 with 3.66% Cu and Alloy 4 with 3.77% Cu, as shown in Fig. 7. In the SAD patterns from [100] zone axis, $T1$ diffraction spots are very apparent, and the corresponding $T1$ precipitates are observed (Figs. 7(c) and (f)). However, θ' streaks become very weak and δ' spots almost disappear (Figs. 7(b) and (e)).

For Alloys 1−4, $T1$ precipitates are the dominant

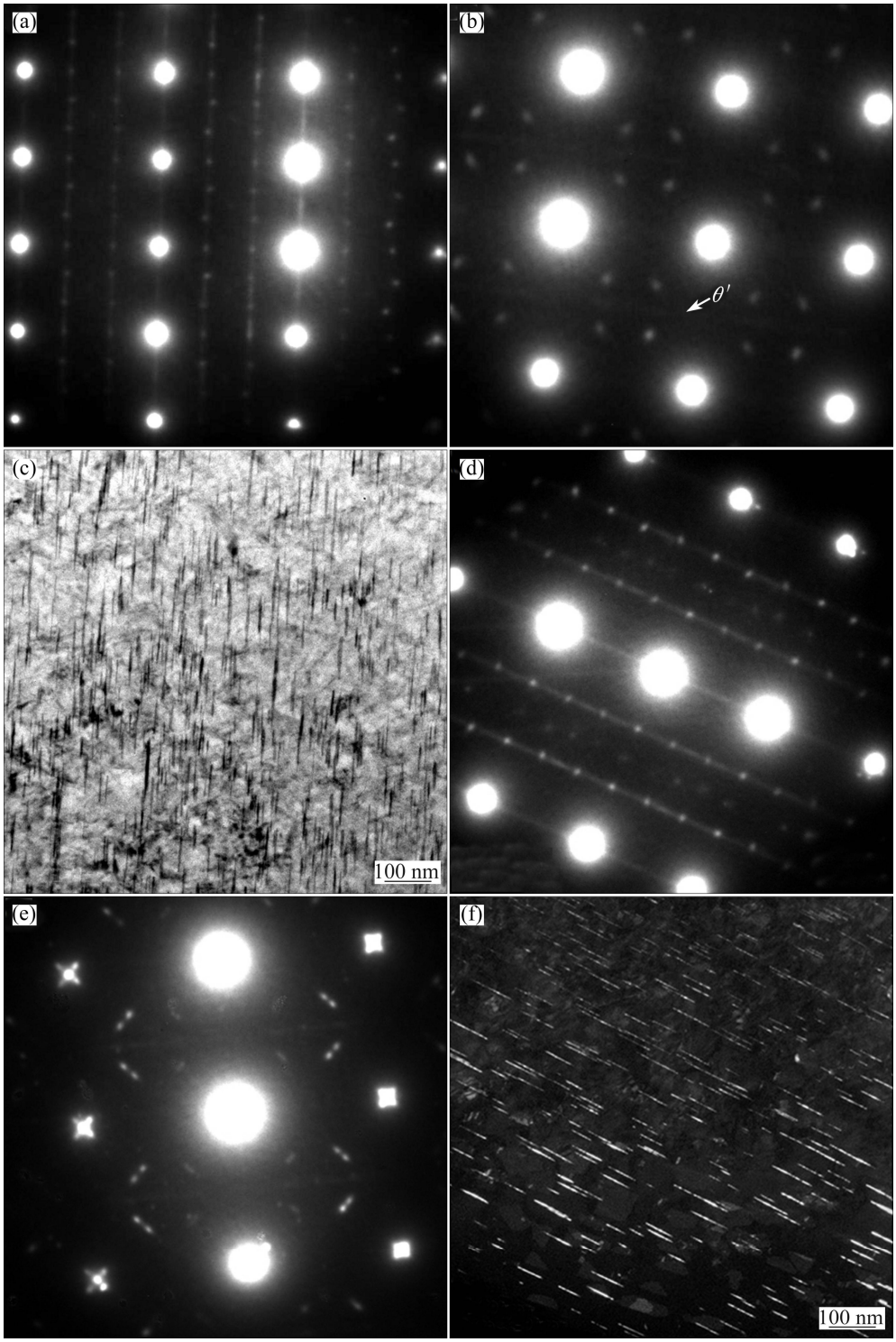

Fig. 7 SAD patterns and DF TEM images of Alloy 3 aged for 20 h (a, b, c) and Alloy 4 aged for 24 h (d, e, f): (a,d) $[112]_{Al}$ SAD patterns; (b,e) $[100]_{Al}$ SAD patterns; (c) $[112]_{Al}$ bright field TEM image showing *T*1 precipitates; (f) $[112]_{Al}$ DF TEM image showing *T*1 precipitates

strengthening phases, minor precipitates of δ' and θ' are also observed. In Alloy 1, the precipitates of δ' and θ' are observed in the under-aging stage (Fig. 4(a)), but almost disappear in the peak-aging stage (Fig. 5(a)). In addition, it seems that for Alloys 1−4, the amount of δ' and θ' precipitates, especially δ' precipitates, becomes smaller, and even disappears as the Cu content increases.

With increasing the Cu content, there is no obvious change in the precipitate types in 1.0% Li-containing Al−Li alloys. However, the variation of Li content results in an obvious change. Figure 8 shows the SAD patterns and DF TEM images of near peak-aged Alloy 5 with

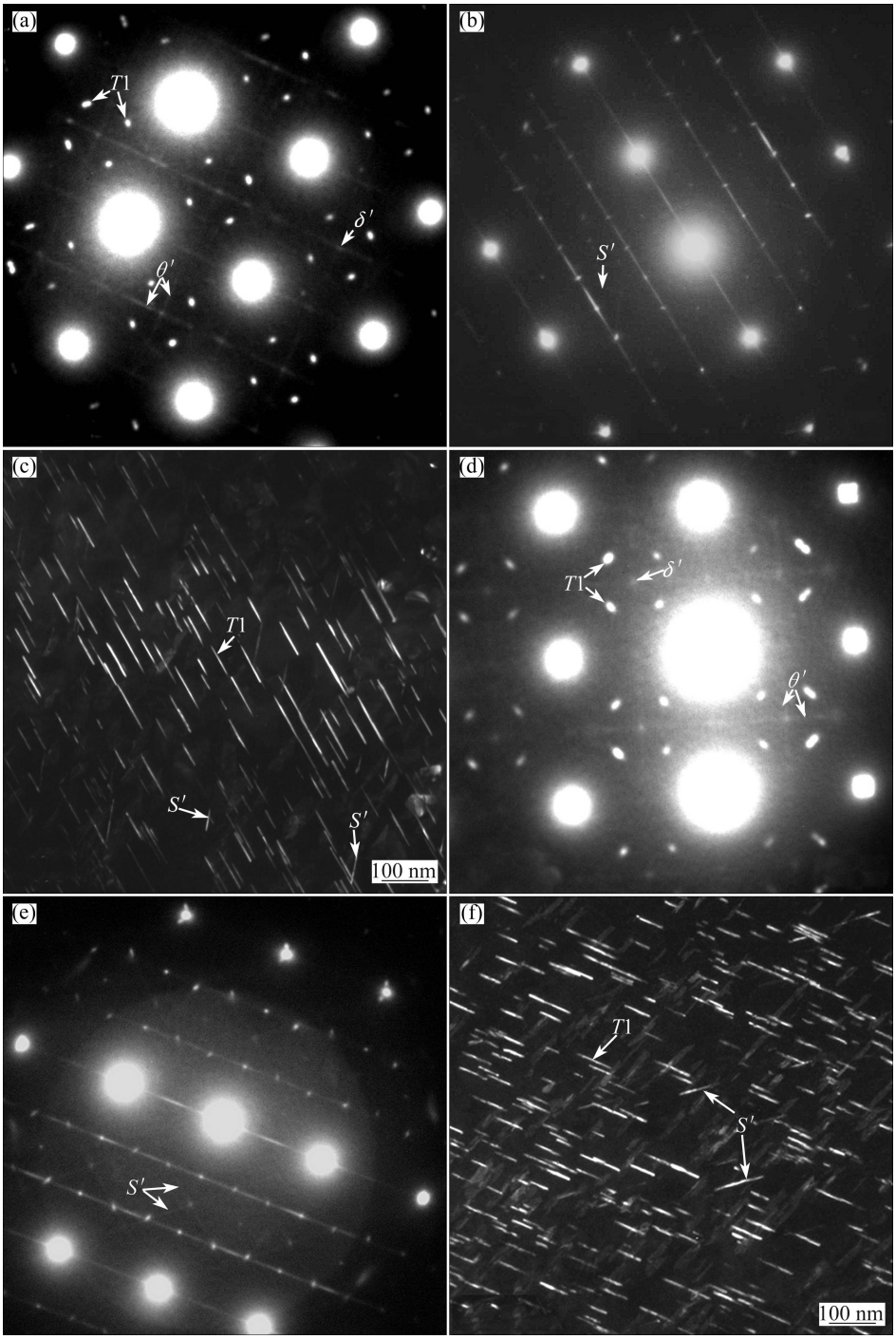

Fig. 8 SAD patterns and TEM images of Alloy 5 aged for 26 h (a, b, c) and Alloy 6 aged for 24 h (d, e, f): (a,d) $[100]_{Al}$ SAD patterns; (b,e) $[112]_{Al}$ SAD patterns; (c,f) $[112]_{Al}$ DF TEM images showing $T1$ precipitates

1.18% Li and Alloy 6 with 1.38% Li. The SAD patterns from [100] zone axis (Figs. 8(a) and (d)) show that the main precipitates are still $T1$ phases in these two alloys. Meanwhile, some δ' and θ' precipitates also appear, their spots or streaks in these two alloys are obviously more intense than those in 1.0% Li-containing Alloy 3 (Fig. 7(b)), which implies that increasing Li content may favor the formation of θ' and δ' precipitates to some extent.

In addition to $T1$, θ' and δ' precipitates, the SAD patterns from [112] zone axis (Figs. 8(b) and (e)) also reveal the presence of a small amount of S' precipitates (see the white arrows). The streaks corresponding to S' precipitates in Alloy 5 (Fig. 8(b)) are weaker than those in Alloy 6 (Fig. 8(e)). Meanwhile, a little more S' precipitates are observed in Alloy 6 (Fig. 7(f)) than in Alloy 5 (Fig. 7(c)). In this case, Mg content of all alloys is kept at about 0.4%, which seems that increasing Li content favors the formation of S' precipitates. There may be two factors that S' phase appears and its

amount increases as the Li content increases. MUKHOPADHYAY and RAO [16] found the phenomenon of poor Mg content in S' phase in an Al−Cu−Mg−Li−Ag alloy and contributed it to the Li atoms substituting for certain amounts of Mg atoms in S' phase. The increase in Li content perhaps provides more Li atoms to substitute for Mg atoms in S' phase, resulting in more S' phase in the matrix. Another possible reason is that increasing Li content favors the formation of δ' precipitates and unstablizes $T1$ precipitates a little [13,17], which makes S' precipitates gain advantages in the precipitation competition.

3.3 Influence of total mole fraction of Cu and Li and their ratio

The strength and microstructures of Al−Cu−Li alloys are dependent on not only the total contents of Cu and Li, but also their ratio, as reported by other researchers [18,19]. Table 2 shows the total mass fraction of Cu and Li as well as their ratio. To discuss the strength dependence, the peak tensile strength of the alloys is also presented. The alloy with greater total mass fraction of Cu and Li and larger ratio possesses higher strength.

Table 2 Total mass fraction of Cu and Li, their ratio and corresponding peak tensile strength of Al−Cu−Li alloys aged at 160 °C in T8 temper

Alloy No.	w(Cu)+w(Li)/%	w(Cu)/w(Li)	Peak tensile strength/MPa
1	4.20	3.375	550
2	4.39	3.480	568
3	4.66	3.660	578
4	4.63	3.927	570
5	4.76	3.034	601
6	5.04	2.702	623
7	4.92	2.417	601

To clearly declare the strength and microstructure dependence on Cu and Li contents, it is more effective to discuss the mole fractions of Cu and Li and their ratio. Cu and Li atoms in the T8-aged Al−Cu−Li alloys exist in two forms, solid solution atoms and non-solution atoms (atoms in precipitates). The difference in strength is mainly influenced by the precipitates containing Cu and Li. Cu and Li atoms exceeding their solubility in the alloy matrix form the precipitates during the aging process. Usually, the solubility of alloying elements of Cu, Li, Mg, Ag and Zn in Al−Cu−Li alloy matrix is dependent on each other. In other words, the solubility of Cu (or Li) in the alloy matrix is decreased due to the solution of Li (or Cu). However, the solubility data of Cu and Li in the Al−Cu−Li alloy matrix are insufficient. In order to simplify the analysis, a simple assumption is made here. Supposing that the solid solubility of Cu and Li at the aging temperature of 160 °C in the Al−Cu−Li alloy matrix is 60% of that taken from the Al−Cu and Al−Li binary phase diagrams. According to Al−Cu and Al−Li phase diagrams, the solid solubility values of Cu and Li are about 0.1% and 0.5% (mass fraction), respectively. The alloy composition is transformed to mole fraction, and the total non-solution mole fraction of Cu and Li and their ratio at the aging temperature of 160 °C are therefore calculated, as shown in Table 3. Meanwhile, the corresponding peak tensile strength of the alloys is also presented.

Table 3 Calculated total non-solution mole fraction of Cu and Li, their ratio and corresponding peak tensile strength of Al−Cu−Li alloys aged at 160 °C in T8 temper

Alloy No.	x(Cu)+x(Li)/%	x(Cu)/x(Li)	Peak tensile strength/MPa
1	3.94	0.438	550
2	4.1	0.546	568
3	4.28	0.570	578
4	4.18	0.623	570
5	4.91	0.444	601
6	5.69	0.371	623
7	5.82	0.333	601

According to Table 3, two phenomena are significant. Firstly, the strength is highly dependent on the non-solution mole fractions of Cu and Li. The tensile strengths of Alloys 5−7 are obviously higher than those of Alloys 1−4, which is corresponding to a much higher total non-solution mole fraction of Cu and Li in Alloys 5−7. Secondly, the non-solution mole ratio Cu and Li is also an important factor, which is especially reflected in the strength variation of Alloys 5−7. Alloys 6 and 7 have a similar total non-solution mole fraction of Cu and Li. However, due to a lower non-solution mole ratio of Cu to Li, the strength of Alloy 7 is lower than that of Alloy 6. In addition, Alloy 7 possesses much higher total non-solution mole fraction of Cu and Li than Alloy 5, but due to a lower non-solution mole ratio of Cu to Li in Alloy 7, its strength is almost the same as that of Alloy 5. The above investigation reveals that the strength of these Al−Cu−Li alloys is under co-control of total non-solution mole fraction of Cu and Li and their ratio. Either total non-solution mole fraction of Cu and Li or their ratio is the dominant factor under different conditions. To develop super-high strength, the total amount of alloying elements of Cu and Li should be increased. Meanwhile, their ratio should also be kept at a certain high level.

The strength dependence is associated with microstructure variation caused by total non-solution mole fraction of Cu and Li and their ratio. The

non-solution Cu and Li atoms form the aging precipitates, such as $T1$, θ' and δ'. As their amounts are increased, the precipitate fraction is accordingly improved, which possibly enhances the alloy strength. In addition, among the precipitates of $T1$, θ' and δ', $T1$ precipitate has a hexagonal crystal structure and a platelet morphology with a main orientation relationship of $\{0001\}_{T1}//\{111\}_{Al}$ and $\langle 1010\rangle_{T1}//\langle 110\rangle_{Al}$ [20]. So, $T1$ precipitates generate a great impediment to the dislocation glide along the $\{111\}_{Al}$ plane and therefore contribute to the strongest strengthening effect, compared with other precipitates like θ' and δ'. According to the microstructure comparison between Alloys 1−4 with higher Cu/Li mole ratios (Figs. 5−7) and Alloys 5 and 6 with lower Cu/Li mole ratios (Fig. 8), higher Cu/Li mole ratio favors the formation of $T1$ precipitates and results in a higher portion of $T1$ phase among all the precipitates. Although the microstructure of Alloy 7 is not observed, it is rational to deduce that Alloy 7 contains lower portion of $T1$ phase than Alloy 6, due to its lower Cu/Li mole ratio. The strength of Alloy 7 is therefore lower than that of Alloy 6.

4 Conclusions

1) As a preliminary exploration for super-high strength Al−Li alloy, the mechanical properties and microstructures of some Mg, Ag and Zn micro-alloyed T8-aged Al−Cu−Li alloys with 3.2%−3.8% Cu and 1.0%−1.4% Li were researched.

2) For alloys with lower Li content of about 1.0%, the strength is not effectively increased with increasing the Cu content. However, the strength can be greatly enhanced by increasing Cu and Li contents simultaneously.

3) The main strengthening precipitates in the Al−Li alloys include $T1$, δ' and θ' phases. With increasing Li content, the fractions of δ' and θ' phases among the precipitates seem to increase a little, and it is also more likely to precipitate S' phase.

4) The strength and microstructure are highly dependent on the total non-solution mole fraction of Cu and Li and their ratio. To obtain super-high strength, the total mole fraction of Cu and Li should be increased, and their ratio should also be kept at a high level.

References

[1] TERRONES L A H, MONTEIRO S N. Composite precipitates in a commercial Al−Li−Cu−Mg−Zr alloy [J]. Mater Charact, 2007, 58(2): 156−161.

[2] IMMARIGEON J P, HOLT R T, KOUL A K, ZHAO L, WALLACE W, BEDDOES J C. Lightweight materials for aircraft applications [J]. Mater Charact, 1995, 35(1): 41−67.

[3] PICKENS J R, HEUBAUM F H, KRAMER L S, LANGAN T J. Ultrahigh strength Al−Cu−Li−Mg alloys: USA, 5259897[P]. 1993−11−09.

[4] RIOJA R J, LIU J. The evolution of Al−Li base products for aerospace and space applications [J]. Metall Mater Trans A, 2012, 43(9): 3325−3337.

[5] ITOH G, CUI Q, KANNO M. Effects of a small addition of magnesium and silver on the precipitation of $T1$ phase in an Al−4%−1.1%Li−0.2%Zr alloy [J]. Mater Sci Eng A, 1996, 211(1−2): 128−137.

[6] CHEN P S, KURUVILLA A K, MALONE T W, STANTON W P. The effects of artificial aging on the microstructure and fracture toughness of Al−Cu−Li alloy 2195 [J]. J Mater Eng Perform, 1998, 7(5): 682−690.

[7] LEQUEU P, SMITH KP, DANIÉLOU A. Aluminum−copper−lithium alloy 2050 developed for medium to thick plate [J]. J Mater Eng Perform, 2010, 19(6): 841−847.

[8] WEI Xiu-yu, ZHENG Zi-qiao, SHE Ling-juan, CHEN Qiu-ni, LI Shi-chen. Micro-alloying roles of Mg and Zn additions in 2099 Al−Li alloy [J]. Rare Mater Eng, 2010, 39(9): 1583−1587. (in Chinese)

[9] DENZER D K, RIOJA R J, BRAY G H, VENERNA G B, COLVIN E L. The evolution of plate and extruded products with high strength and fracture toughness [C]//Proceedings of the 13th International Conference on Aluminum Alloys (ICAA13). Pittsburgh, PA, USA, 2012: 587−592.

[10] LUO Xian-fu, ZHENG Zi-qiao, ZHONG Ji-fa, ZHANG Hai-feng, ZHONG Jing, LI Shi-chen, LI Jin-feng. Effects of Mg, Ag and Zn multialloying on aging behavior of new Al−Cu−Li alloy [J]. The Chinese Journal of Nonferrous Metals, 2013, 23(7): 1833−1842. (in Chinese)

[11] LI Jin-feng, ZHENG Zi-qiao, CHEN Yong-lai, ZHANG Xu-hu. Al−Li alloys and their application in aerospace industry [J]. Aerospace Materials and Technology, 2012, 42(1): 13−19. (in Chinese)

[12] HAGIWARA T, KOBAYASHI K, SAKAMOTO T. Effect of lithium and copper contents on the mechanical properties of Al−Cu−Li alloys [C]//Proceedings of the 4th International Conference on Aluminum Alloys: Their Physical and Mechanical Properties. Atlanta, GA, USA, 1994: 297−304.

[13] KUMAR K S, HEUBAUM F H. The effect of Li content on the natural aging response of Al−Cu−Li−Mg−Ag−Zr alloys [J]. Acta Mater, 1997, 45(6): 2317−2327.

[14] GUPTA R K, NAYAN N, NAGASIREESHA G. Development and characterization of Al−Li alloys [J]. Mater Sci Eng A, 2006, 420(1−2): 228−234.

[15] HERRING R A, GAYLE F W, PICKENS J R. High-resolution electron microscopy study of a high-copper variant of Weldalite 049 and a high-strength Al−Cu−Ag−Mg−Zr alloy [J]. J Mater Sci, 1993, 28(1): 69−73.

[16] MUKHOPADHYAY A K, RAO V V R. Characterization of S (Al_2CuMg) phase particles present in as-cast and annealed Al−Cu−Mg(−Li)−Ag alloys [J]. Mater Sci Eng A, 1999, 268(1−2): 8−14.

[17] MUÑOZ-MORRIS M A, MORRIS D G. Microstructure control during severe plastic deformation of Al−Cu−Li and the influence on strength and ductility [J]. Mater Sci Eng A, 2011, 528(9): 3445−3454.

[18] HYUNG-HO J, HIRANO K. Precipitation processes in Al−Cu−Li alloy studying by DSC [J]. Mater Sci Forum, 1987, 13−14: 377−382.

[19] DECREUS B, DESCHAMPS A, GEUSER F D, DONNADIEU P, SIGLI C, WEYLAND M. The influence of Cu/Li ratio on precipitation in Al−Cu−Li−X alloys [J]. Acta Mater, 2013, 61(6): 2207−2218.

[20] HIROSAWA S, SATO T, KAMIO A. Effects of Mg addition on the kinetics of low temperature precipitation in Al−Li−Cu−Ag−Zr alloys [J]. Mater Sci Eng A, 1998, 242(1−2): 195−201.

Mg、Ag、Zn 多元复合微合金化 Al−(3.2~3.8)Cu−(1.0~1.4)Li 合金的显微组织和力学性能

李劲风[1]，刘平礼[1]，陈永来[2]，张绪虎[2]，郑子樵[1]

1. 中南大学 材料科学与工程学院，长沙 410083；
2. 航天材料及工艺研究所，北京 100076

摘　要：为开发新型超高强铝锂合金，研究 T8 态时效处理的 Mg、Ag、Zn 复合微合金化 Al−(3.2~3.8)Cu−(1.0~1.4)Li 合金的显微组织及力学性能。结果表明，Li 含量较低(1.0%)时，通过增加 Cu 含量来提高铝锂合金强度的作用有限，而同时增加 Cu 和 Li 含量则有利于其强度的明显提高。铝锂合金的主要强化相为大量细小弥散的 $T1(Al_2CuLi)$ 相；同时，合金中还析出少量 $\theta'(Al_2Cu)$相及 $\delta'(Al_3Li)$相，而且随时效过程的进行，其密度降低，甚至消失。Li 含量较高时有利于 δ'相及 θ'相的形成，并可能导致形成少量 $S'(Al_2CuMg)$相。另外，采用非固溶 Cu、Li 原子的总摩尔分数及其比例分析 Cu、Li 含量变化对合金强化效果及显微组织的影响。为获得超高强度的铝锂合金，一方面需提高 Cu、Li 原子的总摩尔分数，另一方面也应维持其较高比例。

关键词：铝锂合金；析出相；Cu/Li 摩尔比；显微组织；力学性能

(Edited by Wei-ping CHEN)